QUARTERLY JOURNAL OF THE ROYAL METEOROLOGICAL SOCIETY
Q. J. R. Meteorol. Soc. **135**: 305–317 (2009)
Published online 26 February 2009 in Wiley InterScience
(www.interscience.wiley.com) DOI: 10.1002/qj.389

Anvil clouds of tropical mesoscale convective systems in monsoon regions

Jasmine Cetrone and Robert A. Houze, Jr.*
Department of Atmospheric Sciences, University of Washington, Seattle, USA

ABSTRACT: The anvil clouds of tropical mesoscale convective systems (MCSs) in West Africa, the Maritime Continent and the Bay of Bengal have been examined with TRMM and CloudSat satellite data and ARM ground-based radar observations. The anvils spreading out from the precipitating cores of MCSs are subdivided into thick, medium and thin portions. The thick portions of anvils show distinct differences from one climatological regime to another. In their upper portions, the thick anvils of West Africa MCSs have a broad, flat histogram of reflectivity, and a maximum of reflectivity in their lower portions. The reflectivity histogram of the Bay of Bengal thick anvils has a sharply peaked distribution of reflectivity at all altitudes with modal values that increase monotonically downward. The reflectivity histogram of the Maritime Continent thick anvils is intermediate between that of the West Africa and Bay of Bengal anvils, consistent with the fact this region comprises a mix of land and ocean influences. It is suggested that the difference between the statistics of the continental and oceanic anvils is related to some combination of two factors: (1) the West African anvils tend to be closely tied to the convective regions of MCSs while the oceanic anvils are more likely to be extending outward from large stratiform precipitation areas of MCSs, and (2) the West African MCSs result from greater buoyancy, so that the convective cells are more likely to produce graupel particles and detrain them into anvils. Copyright © 2009 Royal Meteorological Society

KEY WORDS MCS; TRMM; CloudSat

Received 13 August 2008; Revised 9 January 2009; Accepted 13 January 2009

1. Introduction

In the Tropics, upper-level clouds containing ice and mixtures of ice and liquid water strongly affect the transfer of radiation through the atmosphere. A large proportion of these clouds are associated with deep convection (Pfister *et al.*, 2001; Mace *et al.*, 2006), which generates and lifts hydrometeors to upper levels. Some of these particles fall out quickly as convective showers, while others are detrained to form anvil cloud and/or remain aloft as cirriform cloud after the convective system dies out.

If the deep convection evolves into a larger entity with a precipitation region ∼100 km in dimension, it is called a mesoscale convective system (MCS; Houze, 2004). MCSs often develop a large stratiform precipitation region, and they account for a large fraction of tropical precipitation, anvil cloud and cirrus. Some hydrometeors produced in convective updraughts of an MCS are incorporated into the large mesoscale regions of stratiform precipitation, where they fall out slowly or can be detrained into the environment or left aloft as stratiform anvil. Only a few convective cells are capable of supplying ice to an anvil with large areal extent and thickness (e.g. Houze *et al.*, 2000), and these anvils can exist for many hours. The number, sizes and types of ice particles constituting an anvil produced by convection is determined by the strength and duration of the active convective updraughts as well as by the large-scale vertical motion, environmental wind shear, and moisture profile. These factors also determine how long the anvil is present after convection has ceased (Parsons *et al.*, 1994; Mapes and Zuidema, 1996).

MCSs are major elements of the global circulation. They account for most of the precipitation and latent heating in the tropics. MCSs produce top-heavy latent heating profiles because they have significant stratiform precipitation as well as convective towers (Houze, 1982, 1989). Hartmann *et al.* (1984) and Schumacher *et al.* (2004) have shown that the top-heavy heating profiles of MCSs are felt across the Tropics and must be accurately represented in climate models to accurately explain the mean tropical circulation.

Houze (1982) showed that in addition to producing latent heating, MCSs affect the profile of radiative heating. MCSs produce large anvil clouds that extend outward from the precipitating core. Webster and Stephens (1980) showed that these upper-level ice clouds strongly affect the transfer of short- and long-wave radiation, and Houze (1982) showed that net radiative heating occurs in the upper troposphere as a result of net convergence of long- and short-wave fluxes in the anvil cloud. This net heating at upper levels lasts for many hours after the precipitation

*Correspondence to: Professor Robert Houze, Department of Atmospheric Sciences, University of Washington, Box 351640, Seattle, WA 98195-1640, USA
E-mail: houze@washington.edu

Copyright © 2009 Royal Meteorological Society

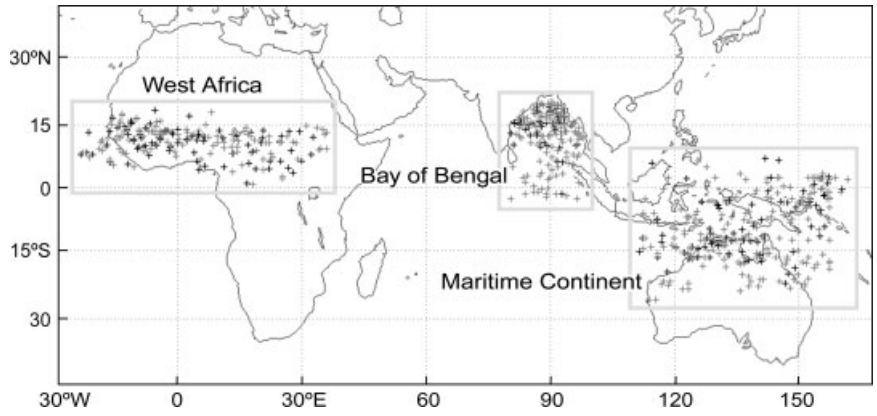

Figure 1. A map of the three regions of interest for this study. The '+' markers are locations of the MCSs identified in this study by TRMM PR (grey) and by CloudSat (black).

has subsided. Clement and Soden (2005) showed that the anvil radiative heating is an important factor in the general circulation. Specifically, they found that a general circulation model is very sensitive to the microphysical processes by which convective cloud systems produce upper-level anvil cloud, and hence modify the radiative heating profile associated with deep convection. Their calculations were based on a convective parametrization (Arakawa and Schubert, 1974) for which the amount of upper-level cloud produced by the convection was determined by arbitrarily adjusting the precipitation efficiency assumed in the parametrization. Their results point out the need to better understand the microphysical mechanisms controlling how the convection produces anvil cloud in MCSs.

Previous studies have developed a conceptual model of MCSs using centimetre wavelength radars (e.g. Houze *et al.*, 1980); however, these methods have concentrated on describing the precipitating regions of these systems. The objective of the study described in this paper is to construct a joint climatology of both the precipitation structure and anvil characteristics of tropical MCSs. The joint climatology indicates the relationship between the precipitation and anvil-forming processes. Tropical MCSs are analyzed over three locations: the Maritime Continent (the region of Indonesia, Malayasia, northern Australia), the Bay of Bengal and West Africa. Climatologies of total precipitation as well as the amount of rain falling from convective and stratiform regions of MCSs are analyzed using data from the Tropical Rainfall Measuring Mission (TRMM) satellite. The structures of anvil clouds of the MCSs are explored using data from the CloudSat satellite (Stephens *et al.*, 2002) and from ground-based vertically pointing radars at the United States Department of Energy Atmospheric Radiation Measurement (ARM) program sites in Australia and Africa. A discussion on how the precipitating regions can affect the generated anvil clouds is also presented.

2. Three Monsoon Regions

Characteristics of both the cloud and precipitation regions in MCSs vary from one tropical location to another. We focus on three different tropical locations notable for MCS occurrence: the Maritime Continent region, the Bay of Bengal, and West Africa (Figure 1). These three regions are among the most impacted by monsoonal precipitation on the planet, and thus are associated with frequent large MCSs during active phases of the monsoon. Additionally, each of the three selected regions has available time-continuous ground- or ship-based precipitation and cloud radar observations. These upward-looking observations are valuable for comparing to the observations obtained by the satellite instruments. As will be shown in section 5.2, these comparisons assure us that the anvil datasets presented herein are not contaminated by attenuation of the radar beams.

The buoyancy over the three regions was estimated using National Centers for Environmental Prediction (NCEP) reanalysis fields of temperature and moisture during the analysis times (described in section 3) and is plotted in Figure 2. Buoyancy here is described as the difference between the environmental temperature and the temperature of a parcel lifted from the 1000 mb level. The 75th percentile of buoyancy is plotted here, as it gives an

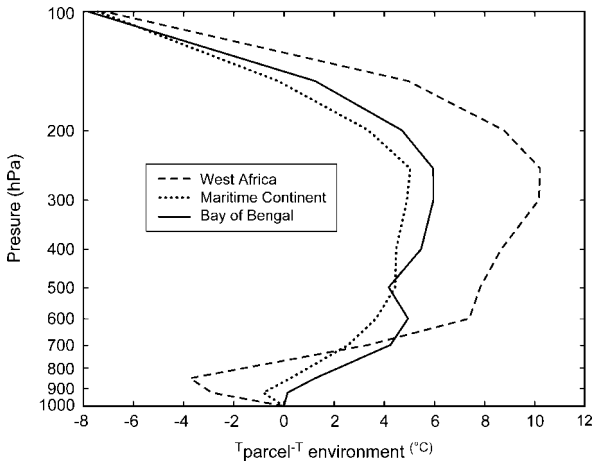

Figure 2. Vertical distribution of the 75th percentile of buoyancy (°C) of a parcel lifted from the 1000 mb level as determined by NCEP reanalysis fields over the three regions of interest.

Copyright © 2009 Royal Meteorological Society

DOI: 10.1002/qj

indication of the greater buoyancy that is likely associated with deeper convection. The differences in buoyancy profiles in the three regions is primarily associated with the shape of the free atmosphere temperature profile. The greatest difference in the free atmospheric soundings is that the African temperature sounding is nearly dry adiabatic in the lower troposphere, while the maritime profiles are nearly moist adiabatic. For this reason, greater buoyancy can be achieved in the West Africa environment, if parcels can overcome significant convective inhibition at the lower levels.

2.1. West Africa

During summer, West Africa is under the influence of its monsoon. The region is a continental monsoon environment and is consistently impacted by large, intense mesoscale convective systems that propagate westward through West Africa during active monsoon conditions (Payne and McGarry, 1977; Fortune, 1980; Houze, 1981; Thorncroft and Hodges, 2001; Schumacher and Houze, 2006; Futyan and DelGenio, 2007). These MCSs can be very intense, electrified, and can create thick anvil clouds. Figure 2 indicates that, in West Africa, once air parcels overcome the considerable convective inhibition (negative buoyancy) at low levels, air parcels lifted beyond about 750 hPa have a strong positive buoyancy throughout much of the troposphere. During the summer of 2006, the African Monsoon Multidisciplinary Analyses (AMMA; Redelsperger *et al.*, 2006) experiment was held. AMMA had many parts, but one location in particular was ideal for this study. At the Niamey site, the ARM program operated a vertically pointing W-band (95 GHz) ARM Cloud Radar (WACR; Mead and Widener, 2005). This radar was used to document the anvils of MCSs over West Africa.

2.2. The Maritime Continent

The Maritime Continent with its islands, peninsulas and intervening oceans is the rainiest region on Earth (Ramage, 1968). Its rainy season extends from November through to March (Hastenrath, 1991) and is connected with both the Asian and Australian monsoons. Winds blowing off the Asian continent and into northern Australia provide large-scale convergence over the region, and MCSs are released by the strong diurnal forcing of land–sea circulations associated with the islands and peninsulas of the region (Houze *et al.*, 1981; Johnson and Houze, 1987; Webster and Houze, 1991; Mapes and Houze, 1992, 1993). These MCSs tend to have large stratiform rain and extensive anvil clouds and cirrus areas (Churchill and Houze, 1984a,b). Figure 2 shows that lifted parcels exhibit moderate positive buoyancy above 900 hPa.

In Darwin, Australia, a long-term dataset has been collected with a vertically pointing cloud radar (frequency 35 GHz) operated by ARM (Moran *et al.*, 1998). This radar was used to document the anvils of MCSs over the Maritime Continent.

2.3. The Bay of Bengal

During active periods of the Asian monsoon, the Bay of Bengal is also impacted by MCSs with large stratiform rain areas and extensive anvil clouds (Houze and Churchill, 1987; Webster *et al.*, 2002; Zuidema, 2003; Houze, 2004; Houze *et al.*, 2007). MCSs occur frequently over the Bay of Bengal both during the pre-monsoon period (May) and the monsoon season from June to September (Wang and LinHo, 2002). Lifted parcels in this region exhibit positive buoyancy through the depth of the troposphere (Figure 2). The buoyancy profile in this region is almost identical to that of the Maritime Continent, although the buoyancy values are slightly higher at all levels.

3. Satellite Data and Methods of Analysis

This study investigates the climatology of precipitation and anvil structures of MCSs over the three regions by examining satellite data obtained from 1 June to 30 September 2006 over West Africa, 1 December 2006 to 15 March 2007 over the Maritime Continent, and 1 June to 30 September 2006 over the Bay of Bengal.

3.1. Identifying TRMM Precipitation Radar data obtained within MCSs

The precipitation data for this study were obtained from the Tropical Rainfall Measuring Mission's (TRMM) Precipitation Radar (PR), the first quantitative spaceborne precipitation radar (Kummerow *et al.*, 1998; Kozu *et al.*, 2001). The TRMM satellite was launched in 1997 and orbits with an inclination of 35°. The PR operates at 13.8 GHz with a 5 km nadir field of view and has had a 245 km swath width since the boost of the satellite, from an altitude of 350 to 402 km, in 2001. The PR operates at the K_u band (2.17 cm wavelength) with a post-boost sensitivity of ~18 dBZ and a vertical resolution of 250 m at nadir. The TRMM data products used in this study are the version 6 qualitative rain characteristics field (TRMM product 2A23) and the gridded, attenuation-corrected three-dimensional reflectivity field (product 2A25). The rain characteristics field includes the categorization of the echo as convective or stratiform (Awaka *et al.*, 1997). The TRMM orbit is not sun-synchronous and samples each region at various times of day.

Because our goal in this paper is to study MCSs, we sample only reflectivities associated with MCSs. A challenging task underlying the success of the study has been to determine which satellite radar observations were obtained in MCSs. To separate the echoes into MCS and non-MCS datasets, hourly infrared geostationary satellite data were used in concert with the PR's reflectivity data (Meteosat-8 over West Africa, MTSAT-1R over the Maritime Continent, Meteosat-5 over the Bay of Bengal). The swath associated with each overpass that sampled over the regions of interest was manually checked for precipitation data; if some were found, they were further

Copyright © 2009 Royal Meteorological Society

DOI: 10.1002/qj

examined to place them in the context of the hourly infrared satellite images. If the precipitation element was associated with an identified MCS on the geostationary infrared satellite, it was included in the study. MCSs were identified on satellite by having a contiguous precipitation region of greater than 100 km in any direction. In the infrared images, precipitation regions were identified as those with brightness temperatures <208 K, which is consistent with the brightness temperature thresholds used previously to identify the active precipitating areas of mesoscale systems in both midlatitudes and Tropics (e.g. Maddox, 1980; Mapes and Houze, 1992; Chen *et al.*, 1996). Significant numbers of MCSs were identified on the PR over the three regions: 120 over West Africa, 190 over the Maritime Continent, and 141 over the Bay of Bengal. The locations of each MCS identified by the TRMM PR are denoted by the grey markers in Figure 1.

3.2. CloudSat Cloud Profiling Radar in MCSs

Data from the anvil clouds produced by MCSs in the three regions were obtained using the CloudSat Cloud Profiling Radar (CPR; Stephens *et al.*, 2002). The CPR has been providing detailed radar reflectivity data since June 2006. It operates at 94 GHz and points nominally in the nadir direction only, with a footprint of approximately 2.5 km along and 1.4 km across track at sea level. The CPR has a sensitivity between −30 and −32 dBZ and a vertical resolution of 480 m (although the signal is oversampled and provides a range gate spacing of 240 m). CloudSat is on a sun-synchronous orbit and passes over each of the regions twice daily (approximately 0000–0130 LT (local time) and 1200–1330 LT, depending on the time zone).

As for the PR data, we examined the CPR data in concert with IR satellite data in order to ensure that the CPR data included in this study were only those obtained within the clouds of MCSs. This subsample of CPR data was then filtered to find only the anvil clouds (non- precipitating portions of clouds associated with MCSs). A cloud was considered to be precipitating if it exceeded −10 dBZ below 5 km (the approximate height of the melting level). The choice of −10 dBZ as precipitating is consistent with ground-based millimetre cloud studies (Stephens and Wood, 2007). This filtering ensured that we were analyzing only anvil clouds. The numbers of MCSs that had anvil sampled by the CPR during our time frame were 82 over West Africa, 78 over the Maritime Continent, and 42 over the smaller Bay of Bengal region. The locations of MCSs identified using CloudSat are denoted by the black markers in Figure 1.

4. Precipitation echo structure

The frequency distribution of reflectivity varies with height, and analysis of this height variation of radar reflectivity can provide insight into the structure and microphysical processes of precipitating cloud systems. In this paper, the statistics of radar reflectivity are represented in Contoured Frequency by Altitude Diagrams (CFADs; Yuter and Houze, 1995). These diagrams are joint probability distributions showing contours representing the frequency of occurrence of a given reflectivity

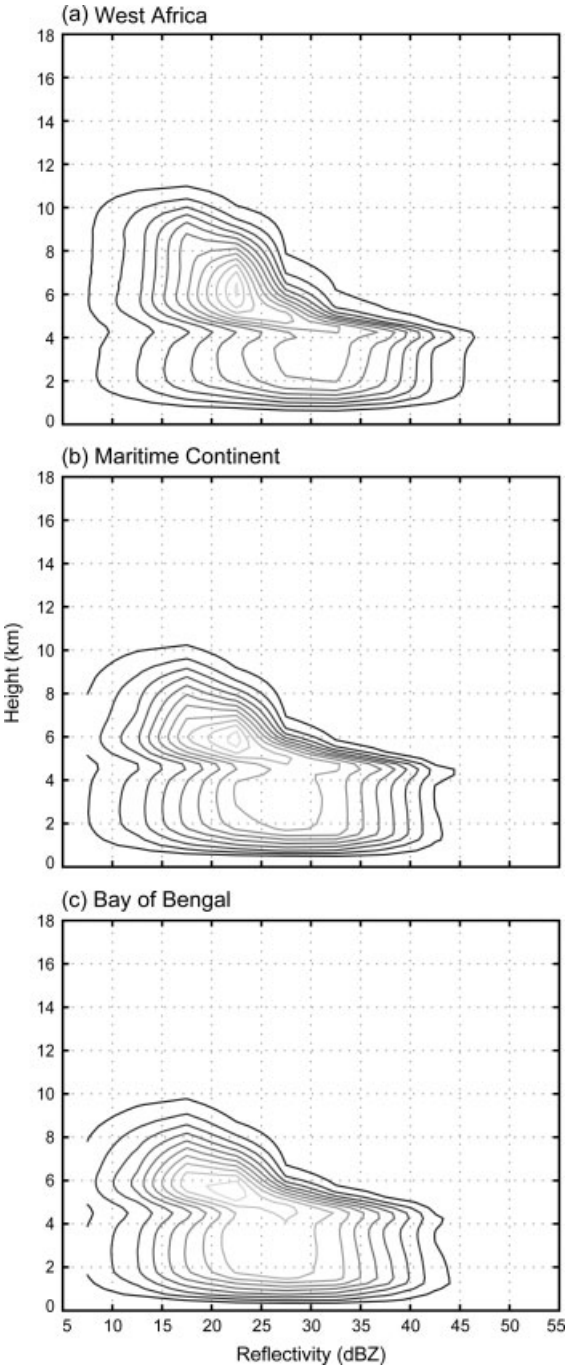

Figure 3. Contoured frequency by altitude diagram (CFAD) showing the frequency distribution of TRMM PR reflectivity as a function of height of MCSs over (a) West Africa, (b) the Maritime Continent and (c) the Bay of Bengal. The contours show bin counts divided by total counts. The contour interval is 0.001 and contour values range from 0.001 to 0.012. Bin dimensions are 5 dBZ by 250 m. The occurrence of reflectivity values lower than the PR sensitivity threshold of 18 dBZ are the result of interpolating the reflectivity data to a Cartesian grid prior to calculating the echo frequency distribution. Houze *et al.* (2007) provides further discussion of the interpolation scheme.

Copyright © 2009 Royal Meteorological Society

DOI: 10.1002/qj

at a given height. The entire distribution was normalized by dividing by the number of samples within the region of analysis to permit the comparison of CFADs between regions despite the difference in the number of samples. CFADs of TRMM PR reflectivity for MCSs over the three regions are shown in Figure 3. (Since TRMM is not sun-synchronous, the time of day of the satellite measurements represented in the CFADs varies.)

The CFADs are characterized by three regimes: above, at, and below the 0 °C level (approximately 5 km). Below 0 °C, echoes are produced by raindrops. The broad distribution of reflectivity values below the 0 °C level indicate that the drops were falling from precipitating entities at a variety of stages of development and/or different intensities. At these levels, West African MCSs (Figure 3(a)) have the highest modal reflectivity, ∼30 dBZ, followed by the Maritime Continent MCSs (Figure 3(b)) at ∼28 dBZ and the Bay of Bengal MCSs (Figure 3(c)) at ∼26 dBZ. The West Africa MCSs appear to have the most spread in reflectivity below the 0 °C level, with echoes reaching peak intensities of 45–46 dBZ, consistent with their greater buoyancy (Figure 2). Both the Bay of Bengal and Maritime Continent MCSs have somewhat lower peak intensities of 43–44 dBZ.

Just below the 0 °C level, the tendency for a melting-level bright band to occur in radar echoes is evident in the CFADs with the shift of the CFAD contours to the right (i.e. toward higher reflectivity values) just below 5 km. This feature is a characteristic of stratiform precipitation CFADs (e.g. Yuter and Houze, 1995; Houze *et al.*, 2007), and its appearance in these CFADs indicates that the echoes in the MCSs of all three regions were a mix of convective and stratiform precipitation.

Above the 0 °C level, the distribution of reflectivity values is much narrower, with a tight gradient of CFAD contours to the right of the peak of the distribution. The echoes of both the Maritime Continent and Bay of Bengal MCSs show a tilting of the CFAD contours toward higher reflectivity values at lower levels. The West Africa MCSs show a somewhat different signature from the other two regions above the 0 °C level. The CFAD has more vertically coherent contours (as opposed to tilting), especially between 5 and 8 km altitude. To better explain some of these features, we separate the TRMM PR radar observations of the precipitation into convective and stratiform components.

The CFADs of precipitation in the convective components of MCSs are shown in Figure 4. Above the 0 °C level, all three distributions show a tilting of the contours toward higher reflectivity values with decreasing height. This tilt indicates the increase of size and concentration of ice particles falling from upper levels. Despite the gross similarities of the three convective CFADs, subtle but important differences are also evident. Figure 4(a) shows that the maximum heights attained by convective echoes of the West African MCSs are much greater than in the other two regions. This behaviour is consistent with the greater potential positive buoyancy in that region (Figure 2). The oceanic MCSs over the Bay of Bengal have the lowest maximum echo heights (Figure 4(c)), while the MCSs over the Maritime Continent (characterized by a land–ocean mix) have maximum echo heights intermediate between the West African and Bay of Bengal MCSs. Below the 0 °C level, the convective precipitation echoes over West Africa have a significantly larger modal reflectivity (∼40 dBZ) compared to the other two regions (∼37 dBZ). This result is again consistent with convection having greater buoyancy and updraught intensity over West Africa

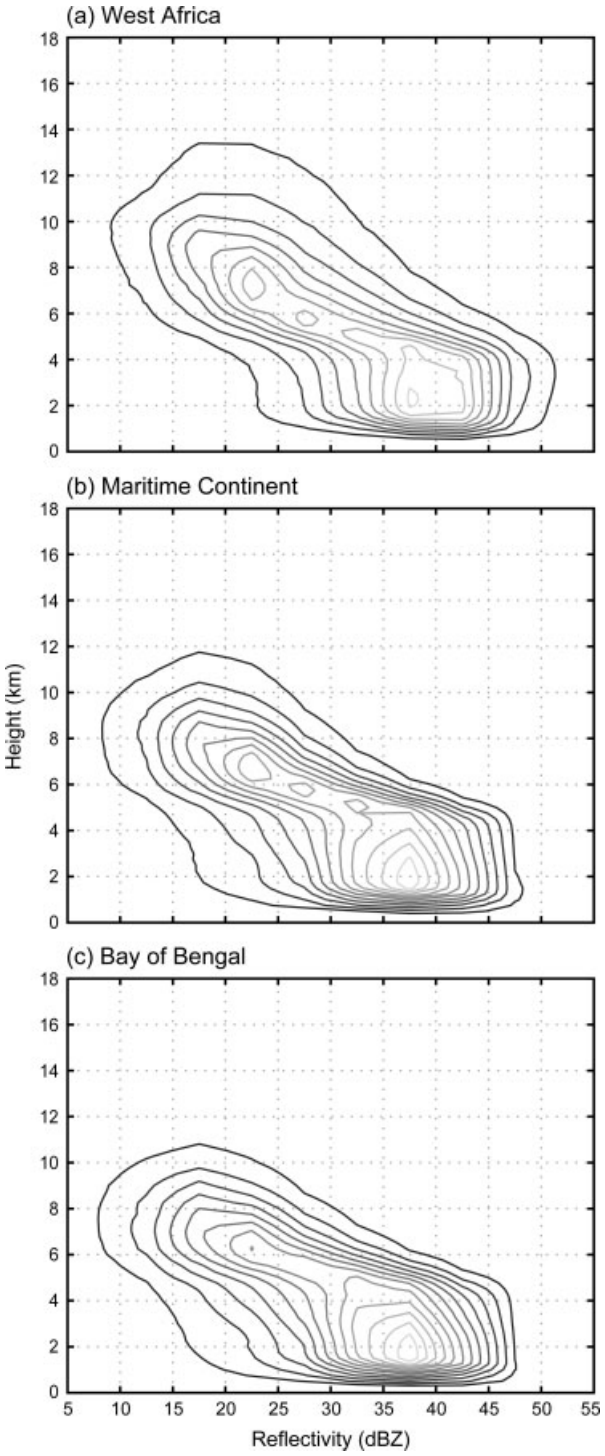

Figure 4. As Figure 3, but for convective echoes.

Copyright © 2009 Royal Meteorological Society

DOI: 10.1002/qj

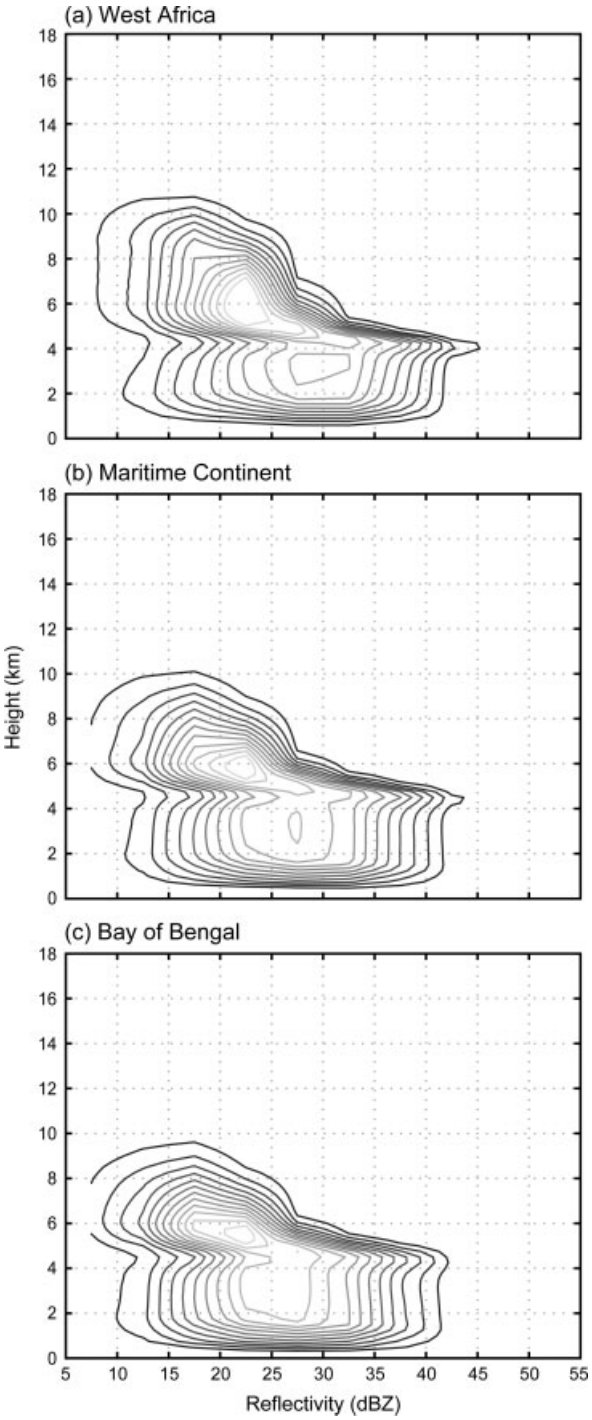

Figure 5. As Figure 3, but for stratiform echoes.

(stronger updraughts lead to larger precipitation particles and heavier rainfall) than the other two regions.

The CFADs of precipitation in the stratiform components of MCSs are shown in Figure 5. All three regions display the same basic CFAD structure. Above the 0 °C level, the tight gradients of the frequency contours are in stark contrast to the looser contour gradients at upper levels in the convective regions (Figure 4). The tight gradients indicate a generally more uniform reflectivity structure at upper levels than in the convective regions. These CFAD characteristics are typical of stratiform region echoes of MCSs (Yuter and Houze, 1995). The stratiform CFADs for the three regions of study exhibit several small but important differences. Like the convective CFADs, the stratiform CFADs show that the maximum heights of echoes associated with West Africa MCSs extend much higher than MCSs in the other two regions. The modal values at all levels above the 0 °C level are greatest in the West African MCSs, which indicates that larger and/or more numerous precipitation particles and higher ice water contents exist above the 0 °C level in West Africa than in the other two regions. These higher reflectivity values probably are a result of ice particles having been originally generated in the convective region and transferred to the stratiform region (Houze *et al.*, 1980; Gamache and Houze, 1983). Below the 0 °C level are further subtle but important differences in the contours among the three regions. The contours of the Bay of Bengal and Maritime Continent stratiform CFADs are generally vertical from just below the bright band down to the surface. The contours of the West Africa CFAD indicate a tendency of lower reflectivity values in echoes near the surface compared to reflectivities just below the bright band. The near-surface environment over West Africa is, on average, very dry compared to the other two regions. This drier environment would be expected to speed up the evaporation of the raindrops as they fall, thus producing a decrease in the returned reflectivity signal at lower levels.

The amount of anvil cloud produced by MCSs is related to the relative amounts of convective and stratiform precipitation occurring in the MCSs. One metric indicating the relative importance of the convective and stratiform components of MCSs is the fraction of the total MCS precipitation area that is identified as convective. The three regions of study do not differ much in either the distribution or mean value of the convective area fraction in these MCSs. In the West Africa MCSs, 16.7% of the echoes are labelled convective, while Maritime Continent and Bay of Bengal MCSs consist of 12.5% and 17.5%, respectively. The lower convective area fraction in the Maritime Continent MCSs is not surprising since these are often massive, long-lasting systems that have very large stratiform areas.

A perhaps more meaningful metric is the surface stratiform rain fraction, which is the fraction of total MCS rain that fell from stratiform echoes. Following Schumacher and Houze (2003), we convert the TRMM PR reflectivity data to rain rate using the TRMM version 6 convective and stratiform near-surface initial reflectivity–rain rate (Z–R) relations ($Z = 148\ R^{1.55}$ and $Z = 276\ R^{1.49}$, respectively). The frequency distributions of stratiform rain fraction over the three regions are shown in Figure 6. The West African MCSs had the most spread in stratiform rain fraction. They had the highest frequency of low stratiform rain fraction of the three regions, and relatively few high stratiform rain fractions. This result is consistent with Schumacher and Houze (2003), who found that stratiform rain fractions tend to be less on average over the African continent than over the ocean. Figure 5 indicates that the stratiform rain in the West

Copyright © 2009 Royal Meteorological Society

DOI: 10.1002/qj

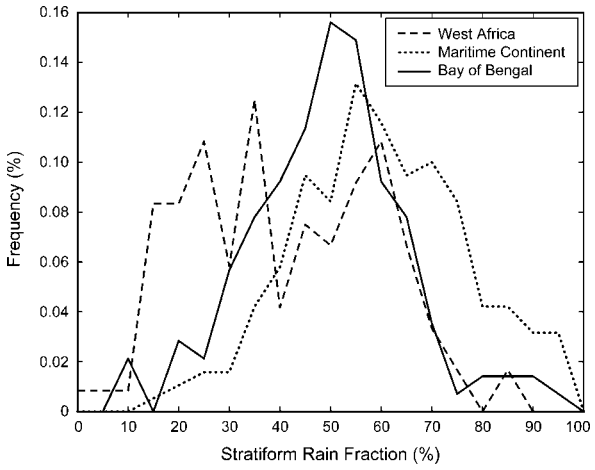

Figure 6. Frequency distribution of the stratiform rain fraction of MCSs as observed by the TRMM PR over the three regions of interest.

Africa MCSs decreased in intensity toward the surface because of evaporation of raindrops below the melting level. The evaporation may partially account for the lower stratiform rain fraction in West Africa. It is also likely that over land some MCSs have shorter life cycles, as a result of convection being shut off by diurnal surface cooling at night. The growth of the stratiform region of an MCS depends on the continual input of condensate by detrainment from the convective cells or by the convective cells dying out and leaving behind stratiform precipitation (Houze, 1997). Unless the deep convection over land can keep forming during the night by some process that counteracts the diurnal cooling, e.g. a low-level moist jet, the MCS cannot be sustained and the stratiform region growth is truncated. Some continental MCSs evolve into long-lasting squall lines (Fortune, 1980; Thorncroft and Hodges, 2001); however, others are undoubtedly truncated in time. The wide spread of stratiform rain fraction values over West Africa (Figure 6) suggests that both long-lived and short-lived MCSs populate the continental region.

In contrast to the West African land mass, tropical oceans are characterized by a weak diurnal cycle, and convection can keep on reforming through the night. As a result, we expect stratiform regions of MCSs to grow more reliably to great size. This difference in MCS 'sustainability' between tropical land and ocean has been suggested previously by Yuter and Houze (1998) and Schumacher and Houze (2003). Being more sustainable, the oceanic MCSs are expected more reliably to have higher stratiform rain fractions. Consistent with this thinking, the Maritime Continent and Bay of Bengal stratiform rain fraction distributions are narrower than that of West Africa in Figure 6. The Maritime Continent has the most frequent occurrence of high stratiform rain fractions (>70%), undoubtedly owing to the influence of the monsoonal systems with massive, long-lasting stratiform regions. The Bay of Bengal MCSs have a stratiform rain fraction distribution similar to that over the Maritime Continent, but shifted to values about 10% lower in rain fraction than the systems over the Maritime Continent.

5. Anvil cloud structure

5.1. CloudSat observations of MCS anvils

5.1.1. Overall anvil structure

As with precipitation echoes, the distribution of anvil radar echo intensities varies with height, so it is useful to create CFAD analyses of the anvil clouds associated with MCSs over the three regions using the CloudSat CPR data (Figure 7). CloudSat samples each location at approximately the same time twice daily (approximately 0000–0130 LT and 1200–1330 LT). The anvil structures that we emphasize below did not vary noticeably between the two sample times in any of the regions. Because of this, and the further fact that we do not know precisely when or where the convection occurred from which the anvils developed, we have not divided the dataset diurnally for the purpose of this paper. Several distinct results emerge from this analysis.

The West African and Maritime Continent anvil CFADs (Figures 7(a), (b)) have a similar distribution of contours. The contours indicate that there is a high frequency of low reflectivity values between 11 and 14 km, with an increase in reflectivity values for lower heights. However, the overall frequency of anvil cloud drops off rapidly for lower heights. The close packing of the contours above the central maximum between 11 and 14 km indicates that there the anvil clouds all have a similar top height, but the spread of contours below that indicates that there are many variations in anvil thickness and cloud density.

The anvil clouds over the Bay of Bengal show a different CFAD structure (Figure 7(c)). The maximum contour values lie in a diagonal starting near the maximum of the other two regions, but extend down to ∼8 km, with higher reflectivity values commonly present at lower heights. This structure indicates an overall tendency for the Bay of Bengal anvils to extend through a deeper layer, with lower cloud bases, than in the other two regions. Also, there is more vertical spread in the contours above ∼12 km than that of the other two regions, indicating that the anvil tops can exist at a wider variety of heights.

The CFADs in Figure 7 further indicate that the anvils over West Africa have systematically lower tops than the other two regions. This is likely caused by a difference in tropopause heights. Hoinka (1998) presented statistics of global tropopause pressures using several different metrics to measure the tropopause. In all of these metrics, the tropopause over West Africa was characterized by a higher pressure (lower height) than both the Bay of Bengal and Maritime Continent regions. It may seem a paradox to have higher convective precipitation echoes over West Africa and lower anvil-top heights; however, maximum convective echo height of the precipitation echoes seen by the TRMM PR (with its sensitivity threshold of ∼+18 dBZ) is moderated by buoyancy and

Copyright © 2009 Royal Meteorological Society

DOI: 10.1002/qj

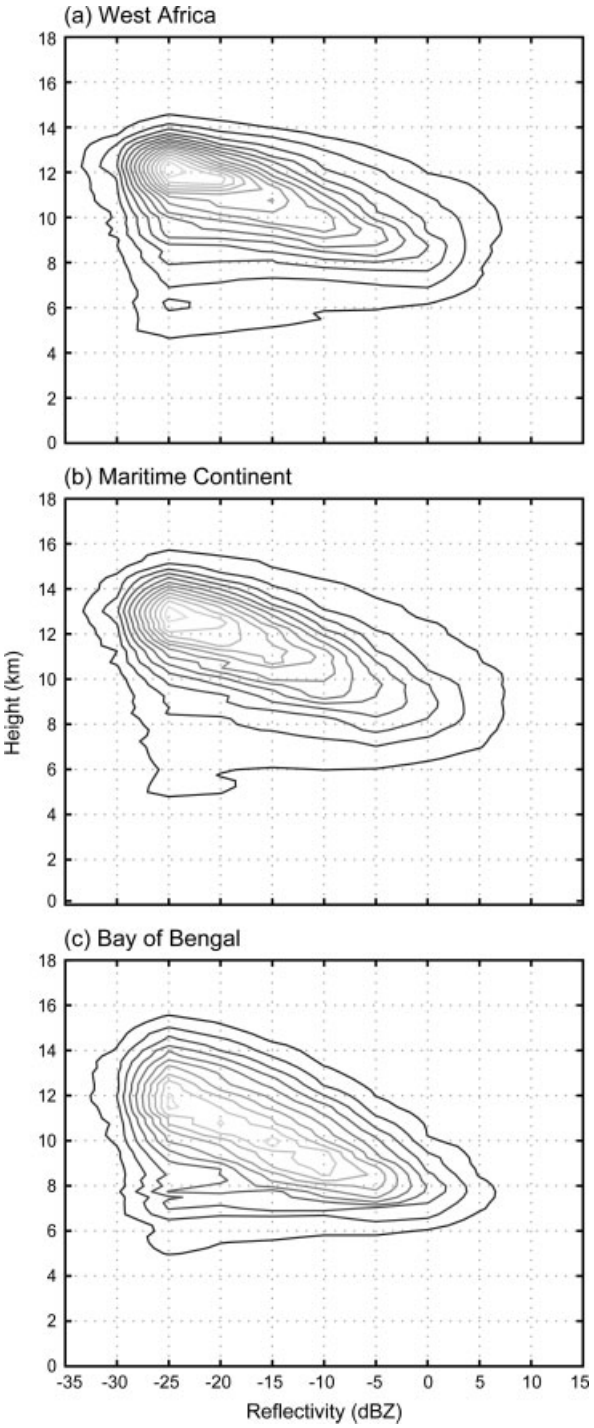

Figure 7. CFAD showing the frequency distribution of CloudSat CPR reflectivity as a function of height of MCS anvil over (a) West Africa, (b) the Maritime Continent and (c) the Bay of Bengal. The contours show bin counts divided by total counts. The contour interval is 0.001 and contour values range from 0.001 to 0.018. Bin dimensions are 5 dBZ by 250m.

vertical motion within the troposphere. The anvil cloud top seen by the much more sensitive CloudSat CPR (with a cutoff of ~ -30 dBZ) is more likely determined by the tropopause height. The differences in anvil-top height among the three regions seen in Figures 7(a)–(c) are consistent throughout the analysis of the CloudSat data.

5.1.2. *Anvils of thin and medium thickness*

The farther the upper-level ice cloud is from the convective cells of the MCS, the thinner the clouds become. It is thus important to subdivide the anvil cloud data according to the thickness of the anvil. We define thin anvil as having a thickness between 0 and 2 km, medium anvil between 2 and 6 km, and thick anvil over 6 km. The distribution of anvil thicknesses over all three regions is dominated by the thinner anvil clouds, and the thin anvils have similar statistics in all three regions. Thin anvils (Figure 8) have very low reflectivity values and tend to

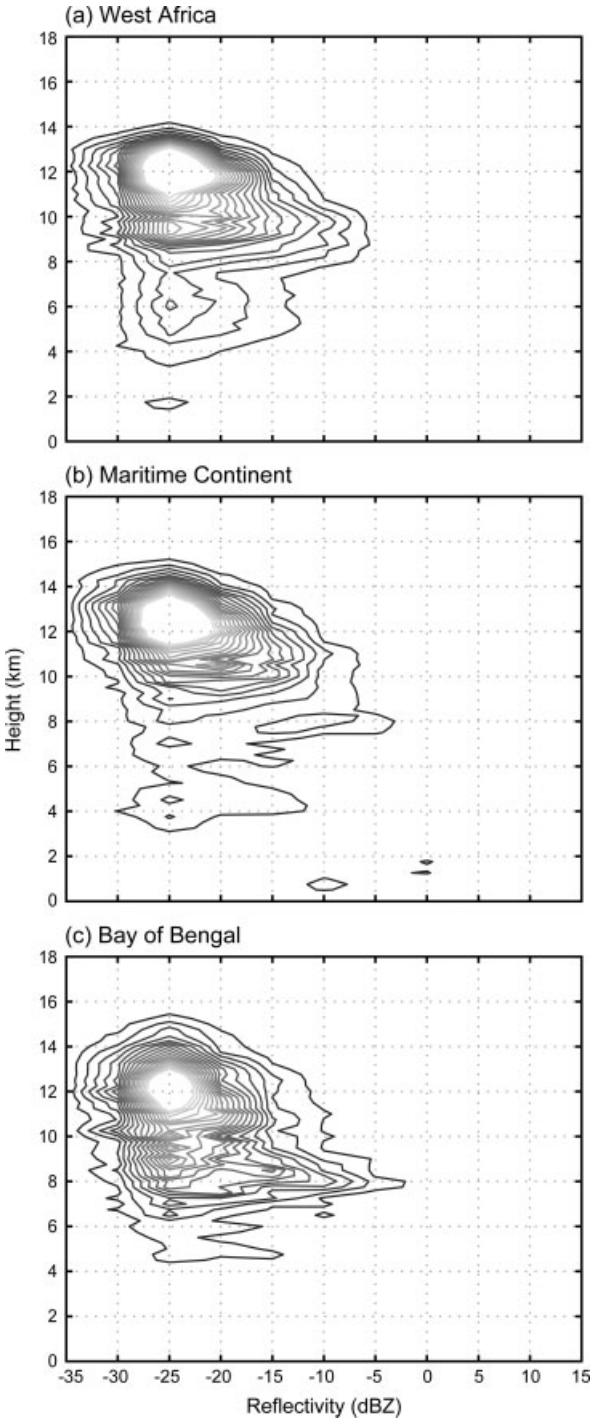

Figure 8. As Figure 7, but for thin ($\leqslant$2 km) anvil.

Copyright © 2009 Royal Meteorological Society

DOI: 10.1002/qj

centre around 12 km for all three regions. Figure 9 shows that the anvils of medium thickness are similar to the overall average CFADs for each region, minus the high-frequency maximum around 12 km (which is an effect of the thin anvil clouds).

5.1.3. *Thick anvils*

The CFADs associated with the thick anvil clouds show several pronounced signatures (Figure 10). In their upper portions, the thick anvils of West Africa MCSs have a broad, flat distribution of reflectivity (Figure 10(a)). Their most frequently occurring reflectivity shown is ∼0 dBZ, occurring at ∼8 km, in the lower portion of the anvil. The CFAD of the Bay of Bengal thick anvils (Figure 10(c)) is very different; in this dataset they tend to be less reflective (the most frequently occurring reflectivity ∼−5 dBZ at ∼9 km), and they have a sharply peaked distribution of reflectivity at all levels with modal values that increase monotonically downward. The CFAD of the Maritime Continent thick anvils (Figure 10(b)) is between that of the West Africa and Bay of Bengal anvils, consistent with the fact that the West Africa convection is continental, the

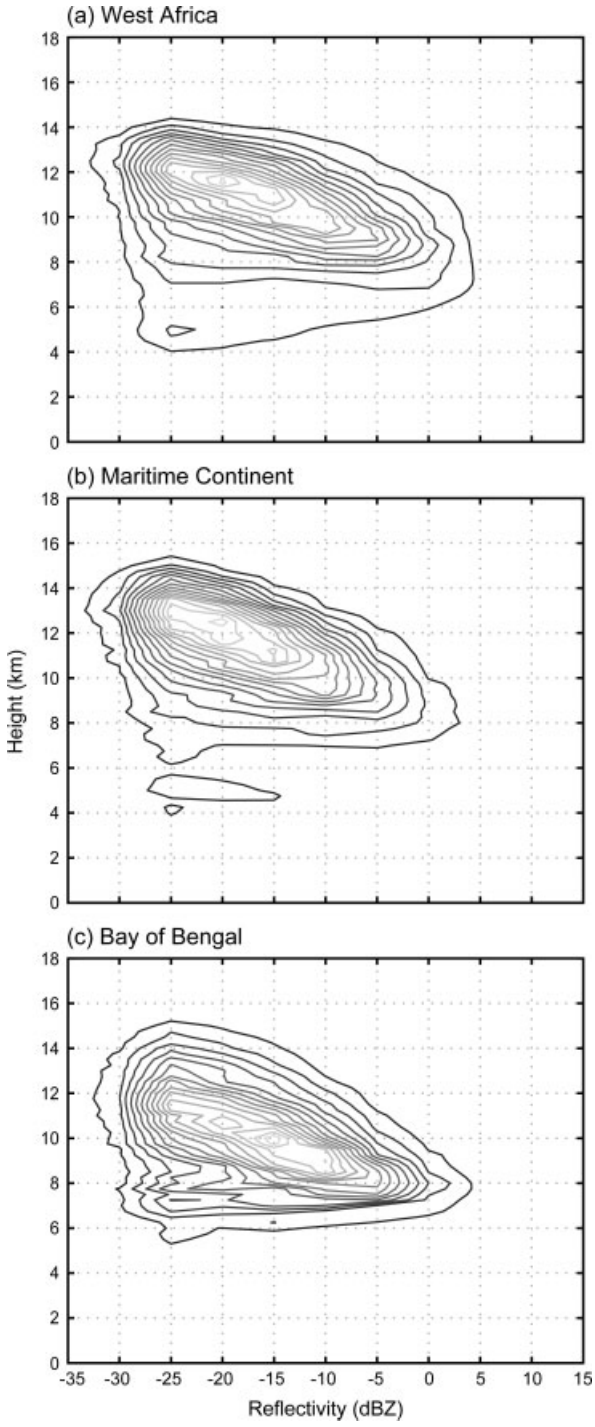

Figure 9. As Figure 7, but for medium(>2 km and ⩽6 km) anvil.

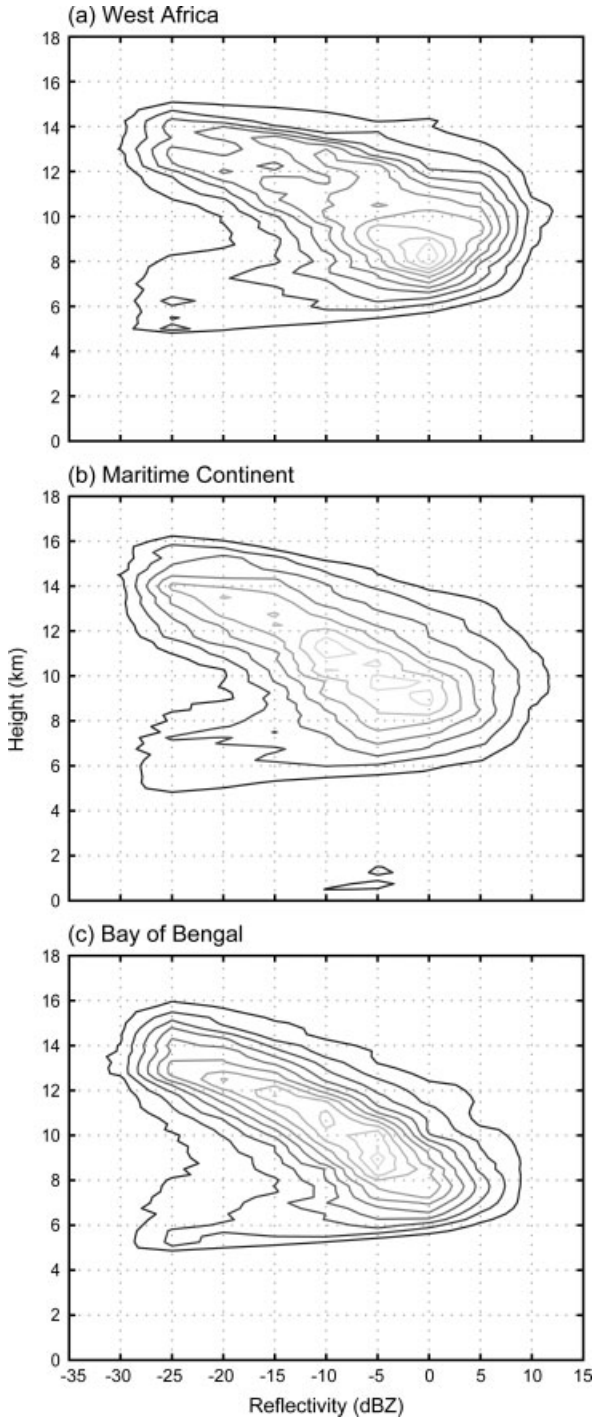

Figure 10. Same as Figure 7, but for thick (>6 km) anvil.

Copyright © 2009 Royal Meteorological Society

DOI: 10.1002/qj

Bay of Bengal convection is oceanic, and the Maritime continent is a mix of land and ocean convection.

We examine the difference between the continental and oceanic thick anvils by comparing the CFADs for West Africa (Figure 10(a)) and the Bay of Bengal (Figure 10(c)). West Africa on average has a lower stratiform rain fraction that the Bay of Bengal and other tropical oceanic regions (Schumacher and Houze, 2003). The Bay of Bengal has MCSs with enormous stratiform rain regions (Houze and Churchill, 1987; Houze *et al.*, 2007). The odds would therefore suggest that the anvils of Bay of Bengal MCSs would frequently extend outward from large precipitating stratiform regions, while the West African anvils would often be less extensive and more directly attached to their originating deep convective elements. Exceptions occur; West Africa is well known for robust, long-lasting squall lines with wide trailing stratiform regions (Hamilton and Archbold, 1945; Fortune, 1980; Thorncroft and Hodges, 2001; Schumacher and Houze, 2006; Futyan and DelGenio, 2007). However, as illustrated by Schumacher and Houze (2006), a number of West Africa MCSs have much more horizontally limited anvils that are directly attached to convective cells, and the overall statistics in the CFAD of Figure 10(a) are likely to have included a number of these cases.

Yuter and Houze (1995) and Houze *et al.* (2007) show that, in the precipitating regions of MCSs, the convective regions have broad, relatively flat histograms of reflectivity at upper levels consistent with a highly variable convective-cell structure, while stratiform precipitation regions have narrow, sharp distributions of reflectivity with modal values increasing monotonically downward. The flatter distribution of reflectivity at upper levels of the West Africa thick anvils shown by the CFAD in Figure 10(a) is consistent with these thick anvils being the residue of deep precipitating cells that produce a broad flat distribution of reflectivity. The Bay of Bengal thick anvil CFAD in Figure 10(b), which shows sharp distributions indicating homogeneous anvil structure at all levels and more frequent extension to lower levels, has a structure similar to the stratiform precipitation region anvils seen by Yuter and Houze (1995) and Houze *et al.* (2007). This similarity is consistent with these thick anvils extending outward from broad stratiform regions of oceanic MCSs. Yuter and Houze (1995) associated this type of CFAD structure with uniform stratiform structures above the 0 °C level, where ice particles are envisioned to be drifting down and systematically growing by vapour deposition and ice particle aggregation to form larger-sized particles as they approach the lower part of the ice cloud. In the Monsoon Experiment (MONEX), research flights were conducted in anvils of MCSs over the Bay of Bengal and the oceanic regions of the Maritime Continent (Churchill and Houze, 1984a,b; Houze and Churchill, 1987). These flights showed ice particle types at all levels in the cloud that were entirely consistent with ice particles drifting down and growing by vapour diffusion.

The MONEX flights further showed no evidence of graupel in the anvil clouds of the oceanic MCSs of the Bay of Bengal and Maritime Continent. The greater buoyancy over the West African continent (Figure 2) indicates that stronger updraughts would occur there than over the oceanic regions and that these updraughts would be more likely to produce larger graupel particles. The fact that tropical Africa has an extremely high frequency of lightning (Christian *et al.*, 2003; Houze, 2004; Cecil *et al.*, 2005) is a clear indication that the MCSs in this region contain graupel. Graupel has higher fall velocities than smaller, less rimed ice particles (Houze, 1993). The heavy rapidly falling graupel particles would have been harder to loft all they way to the tops of convective cells and were likely ejected from the convective updraughts into the anvil well below cloud top. This characteristic of the West Africa convection could account for the strong peak of high reflectivity in the lower portions of the West Africa thick anvils (Figure 10(a)).

5.2. Ground-based ARM cloud radar observations of thick anvils

As noted in sections 2.1 and 2.2, the ARM Program collected ground-based millimetre cloud radar data at two of the three regions of study, Niamey in West Africa and Darwin in the Maritime Continent. The Darwin Millimeter Wavelength Cloud Radar (MMCR) operates at a frequency of 35 GHz. During the summer of 2006, the ARM Mobile Facility at Niamey, Niger, deployed the WACR, which operates at a frequency of 95 GHz. The anvils from MCSs that passed over the ARM cloud radars at both locations have been analyzed. The thick anvil CFADs are plotted in Figure 11. Exact quantitative comparisons with the CloudSat CFADs in Figure 10 cannot be achieved because of the difference in radar calibrations and sensitivities (the WACR is more sensitive to small particles). However, the structures of the CFADs nonetheless contain a wealth of information.

The general structure of the ground-based CFADs for thick anvils in Figure 11 is remarkably similar to that of the CloudSat CFADs in Figure 10. The ground-based CFADs all show the maximum frequency at higher reflectivity in the lower part of the anvil ($\sim$8–10 km altitude). The similarity of structure between the CFADs of the upward-looking ground-based radars and the downward-looking CloudSat CPR show that the anvil structures seen by both types of instruments are robust, and that neither type of radar data is contaminated by beam attenuation.

The CFAD associated with thick anvils sampled by the WACR in Niamey (Figure 11(a)) is very similar to that sampled by the CloudSat CPR over West Africa (Figure 10(a)). The high frequency of higher-reflectivity values appears as well as the lower frequency of low dBZ values. The thick anvils sampled by ground-based radar at Darwin have some differences from the satellite-based CFADs over the general region of the Maritime Continent (cf. Figures 10(b) and 11(b)). These differences are likely due to the occurrence of a particular mode of precipitation that is more frequent over Darwin than the Maritime Continent as a whole. The higher frequencies appear to be

Copyright © 2009 Royal Meteorological Society

DOI: 10.1002/qj

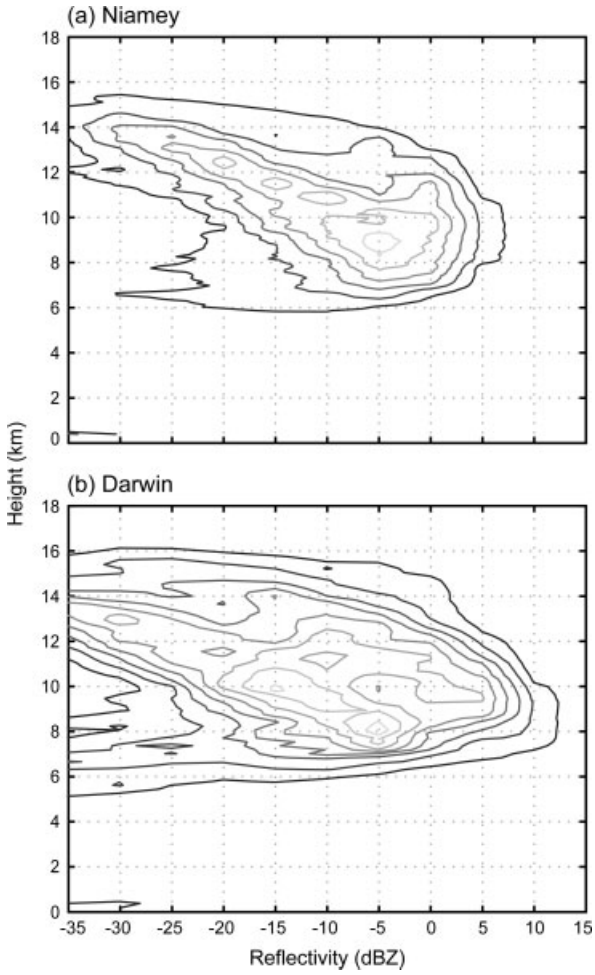

Figure 11. CFAD showing the frequency distribution of reflectivity as a function of height of MCS anvil as observed by ARM ground-based cloud radars: (a) the WACR radar in Niamey, Niger and (b) the MMCR radar in Darwin, Australia. The contours show bin counts divided by total counts. The contour interval is 0.001 and contour values range from 0.001 to 0.018. Bin dimensions are (a) 5 dBZ by 42m, and (b) 5 dBZ by 88m.

similar to those observed by the CPR over the Maritime Continent. However, there appears to be a secondary maximum in frequencies starting at approximately 2.5 dBZ at 9.5 km in altitude and decreasing in intensity with height up to 12 km, where it merges with the first maximum. It thus appears that the presence of higher reflectivity anvils occurs more often in Darwin than over the Maritime Continent as a whole, likely due to the influence of continentally driven MCSs that propagate past Darwin during breaks in the monsoon.

Although there are a few differences in the CFADs between the ground-based and satellite-based instruments, the overwhelming consistency of the two data sources indicates that climatological studies of the anvil structure from satellite data can be assumed to be representative of radar data obtained viewing the anvils from a ground-based perspective. One of the limitations of the satellite data is that the processes of formation of the anvils cannot be easily deduced because of the lack of mesoscale time continuity. The similarity of the ground-based and satellite CFADs for thick anvils indicates that physical understanding of satellite-based anvil climatologies can be achieved via case-studies of time-continuous ground-based radar data.

6. Conclusions

In general, the anvils generated by the MCSs in West Africa, the Maritime Continent, and the Bay of Bengal all have similar statistics. Figure 7 shows that the overall anvil CFAD structure has only small differences among the three regions. However, these statistics are dominated by the large numbers of measurements of the extensive thin portions of MCS anvils (defined as those parts of anvils that are 0–2 km in vertical dimension). The thin anvil clouds are generally located at about the 12 km level and nearly identical in structure on radar. The portions of anvil clouds that are of medium (2–6 km) depth also have very similar structures in all venues (Figure 9).

Most of the variation in anvil structure among MCSs is evident in the thick (>6 km in vertical dimension) portions of anvils. The CFAD of West Africa thick anvils (Figure 10(a)) shows a broad, flat histogram of reflectivity, and a maximum of reflectivity in the lower reaches of the anvils. In contrast, the CFAD of the Bay of Bengal thick anvils has a sharply peaked distribution of reflectivity at all altitudes with modal values that increase monotonically downward. The reflectivity histogram of the Maritime Continent thick anvils is intermediate between that of the West Africa and Bay of Bengal anvils, consistent with the fact this region comprises a mix of land and ocean influences. This observed difference between the statistics of the continental and oceanic anvils implies that future parametrizations and representations of anvil clouds in climate and numerical prediction models will have to be flexible enough to account for different anvil physics in the two regions. The difference between the statistics of the continental and oceanic anvils needs to be better understood, but appears to be related to some combination of two factors:

(1) the West African anvils tend to be closely tied to the convective regions of MCSs while the oceanic anvils are more likely to be extending outward from large stratiform precipitation areas of MCSs, and
(2) the West African MCSs result from greater buoyancy (Figure 2). Consequently, the precipitating cores are deeper and have heavier rain (Figure 4), and stronger convective updraughts almost certainly produce copious graupel, which has higher fall velocities than smaller, less rimed ice particles and would therefore be likely to fall out of or be detrained from the updraught cell before being lofted to cloud top.

The overall statistics of the thick anvils from the West Africa and Maritime Continent regions look the same in satellite (CloudSat) and ground-based radar data (Figure 11). This agreement not only gives a ground-up verification of the satellite climatologies, but

Copyright © 2009 Royal Meteorological Society

DOI: 10.1002/qj

also indicates that time-continuous case-studies based on upward-pointing cloud radars in these regions will help give a physical understanding of the satellite-based observations. A follow-up paper will explore cases for which time-continuous data from ground-based cloud and precipitation radars will be used to test the ideas generated by the data presented in the present paper. In addition, high-resolution simulation by cloud-resolving models will be necessary to fully understand the microphysical mechanisms of the anvil generation by MCSs, as well as to determine the three-dimensional water budget of these systems.

Acknowledgements

This research was supported by the following grants: ARM-DOE grant DE-FG02-06ER64175, NASA grant NNX07AQ89G, NASA ESSF award NNG05GP07H and NASA PMM grant NNX07AD59G. Valuable data processing assistance was provided by Stacy Brodzik. The authors would like to thank Ed Zipser for his helpful comments. The figures were edited and refined by Beth Tully.

References

Arakawa A, Schubert W. 1974. Interaction of a cumulus cloud ensemble with the large-scale environment. *J. Atmos. Sci.* **35**: 674–701.

Awaka J, Iguchi T, Kumagai H, Okamoto K. 1997. Rain type classification algorithm for TRMM Precipitation Radar. In Proceedings of International Geoscience and Remote Sensing Symposium, 3–8 August 1997, Singapore. *IEEE Trans. Geosci. Remote Sensing* **4**: 1633–1635.

Cecil DJ, Goodman SJ, Boccippio DJ, Zipser EJ, Nesbitt SW. 2005. Three years of TRMM precipitation features. Part 1: Radar, radiometric, and lightning characteristics. *Mon. Weather Rev.* **133**: 543–566.

Chen SS, Houze RA Jr, Mapes BE. 1996. Multiscale variability of deep convection in relation to large-scale circulation in TOGA COARE. *J. Atmos. Sci.* **53**: 1380–1409.

Churchill DD, Houze RA Jr. 1984a. Development and structure of winter monsoon cloud clusters on 10 December 1978. *J. Atmos. Sci.* **41**: 933–960.

Churchill DD, Houze RA Jr. 1984b. Mesoscale updraught magnitude and cloud-ice content deduced from the ice budget of the stratiform region of a tropical cloud cluster. *J. Atmos. Sci.* **41**: 1717–1725.

Christian HJ, Blakeslee RJ, Boccippio DJ, Boeck WL, Buechler DE, Driscoll KT, Goodman SJ, Hall JM, Koshak WJ, Mach DM, Stewart MF. 2003. Global frequency and distribution of lightning as observed from space by the Optical Transient Detector. *J. Geophys. Res.* **108**: 4005, DOI: 10.1029/2002JD002347.

Clement AC, Soden B. 2005. The sensitivity of the tropical-mean radiation budget. *J. Climate* **14**: 3189–3203.

Fortune M. 1980. Properties of African squall lines inferred from time-lapse satellite imagery. *Mon. Weather Rev.* **108**: 153–168.

Futyan J, Del Genio A. 2007. Deep convective system evolution over Africa and the tropical Atlantic. *J. Climate* **20**: 5041–5060.

Gamache JF, Houze RA Jr. 1983. Water budget of a mesoscale convective system in the tropics. *J. Atmos. Sci.* **40**: 1835–1850.

Hamilton RA, Archbold JW. 1945. Meteorology of Nigeria and adjacent territory. *Q. J. R. Meteorol. Soc.* **71**: 231–264.

Hartmann DL, Hendon HH, Houze RA Jr. 1984. Some implications of the mesoscale circulations in tropical cloud clusters for large-scale dynamics and climate. *J. Atmos. Sci.* **41**: 113–121.

Hastenrath S. 1991. *Climate Dynamics of the Tropics.* Kluwer Academic Publishers: Dordrecht.

Hoinka KP. 1998. Statistics of the global tropopause pressure. *Mon. Weather Rev.* **126**: 3303–3325.

Houze RA Jr. 1981. Structures of atmospheric precipitation systems–A global survey. *Radio Science* **16**: 671–689.

Houze RA Jr. 1982. Cloud clusters and large-scale vertical motions in the tropics. *J. Meteorol. Soc. Japan* **60**: 396–410.

Houze RA Jr. 1989. Observed structure of mesoscale convective systems and implications for large-scale heating. *Q. J. R. Meteorol. Soc.* **115**: 425–461.

Houze RA Jr. 1993. *Cloud Dynamics*. Academic Press: San Diego.

Houze RA Jr. 1997. Stratiform precipitation in regions of convection: A meteorological paradox? *Bull. Am. Meteorol. Soc.* **78**: 2179–2196.

Houze RA Jr. 2004. Mesoscale convective systems. *Rev. Geophys.* **42**: 10.1029/2004RG000150.

Houze RA Jr, Churchill DD. 1987. Mesoscale organization and cloud microphysics in a Bay of Bengal depression. *J. Atmos. Sci.* **44**: 1845–1867.

Houze RA Jr, Cheng C-P, Leary CA, Gamache JF. 1980. Diagnosis of cloud mass and heat fluxes from radar and synoptic data. *J. Atmos. Sci.* **37**: 754–773.

Houze RA Jr, Geotis SG, Marks FD Jr, Churchill DD, Herzegh PH. 1981. Comparison of airborne and land-based radar measurements of precipitation during winter MONEX. *J. Appl. Meteorol.* **20**: 772–783.

Houze RA Jr, Chen SS, Kingsmill DE, Serra Y, Yuter SE. 2000. Convection over the Pacific warm pool in relation to the atmospheric Kelvin-Rossby wave. *J. Atmos. Sci.* **57**: 3058–3089.

Houze RA Jr, Wilton DC, Smull BF. 2007. Monsoon convection in the Himalayan region as seen by the TRMM Precipitation Radar. *Q. J. R. Meteorol. Soc.* **133**: 1389–1411.

Johnson RH, Houze RA Jr. 1987. Precipitating cloud systems of the Asian monsoon. Pp. 298–353 in *Monsoon Meteorology*. *Oxford Monographs on Geology and Geophysics* No. 7. Chang C-P, Krishnamurti TN (eds.) Oxford University Press: New York.

Kozu T, Kawanishi T, Kuroiwa H, Kojima M, Oikawa K, Kumagai H, Okamoto K, Okumura M, Nakatsuka H, Nishikawa K. 2001. Development of precipitation radar onboard the Tropical Rainfall Measuring Mission (TRMM) satellite. *IEEE Trans. Geosci. Remote Sens.* **39**: 102–116.

Kummerow C, Barnes W, Kozu T, Shiue J, Simpson J. 1998. The Tropical Rainfall Measuring Mission (TRMM) sensor package. *J. Atmos. Oceanic Technol.* **15**: 809–817.

Mace GG, Deng M, Soden B, Zipser E. 2006. Association of tropical cirrus in the 10–15-km layer with deep convective sources: An observational study combining millimeter radar data and satellite-derived trajectories. *J. Atmos. Sci.* **63**: 480–503.

Maddox RA. 1980. Mesoscale convective complexes. *Bull. Am. Meteorol. Soc.* **61**: 1374–1387.

Mapes BE, Houze RA Jr. 1992. 'Satellite-observed cloud clusters in the TOGA-COARE domain'. *TOGA Notes*, April 1992, 5–8. http://www.atmos.washington.edu/MG/PDFs/TOGA92_mape_satellite.pdf.

Mapes BE, Houze RA Jr. 1993. An integrated view of the 1987 Australian monsoon and its mesoscale convective systems. Part II: Vertical structure. *Q. J. R. Meteorol. Soc.* **119**: 733–754.

Mapes BE, Zuidema P. 1996. Radiative-dynamical consequences of dry tongues in the tropical troposphere. *J. Atmos. Sci.* **53**: 610–638.

Mead JB, Widener KB. 2005. 'W-Band ARM cloud radar'. Proceedings of 32nd Conf. on Radar Meteorology, Albuquerque. American Meteorological Society: Boston.

Moran KP, Martner BE, Post MJ, Kropfli RA, Welsh DC, Widener KB. 1998. An unattended cloud profiling radar for use in climate research. *Bull. Am. Meteorol. Soc.* **79**: 443–455.

Parsons D, Dabberdt W, Cole H, Hock T, Martin C, Barrett A-L, Miller E, Spowart M, Howard M, Ecklund W, Carter D, Gage K, Wilson J. 1994. The integrated sounding system: Description and preliminary observations from TOGA-COARE. *Bull. Am. Meteorol. Soc.* **75**: 553–569.

Payne SW, McGarry MM. 1977. The relationship of satellite inferred convective activity to easterly waves over West Africa and the adjacent ocean during phase III of GATE. *Mon. Weather Rev.* **105**: 413–420.

Pfister L, Selkirk HB, Jensen EJ, Schoeberl MR, Toon OB, Browell EV, Grant WB, Gary B, Mahoney MJ, Bui TV, Hintsa E. 2001. Aircraft observation of thin cirrus clouds near the tropical tropopause. *J. Geophys. Res.* **106**: 9765–9786.

Ramage CS. 1968. Role of a tropical 'Maritime Continent' in the atmospheric circulation. *Mon. Weather Rev.* **96**: 365–370.

Redelsperger JL, Thorncroft CD, Diedhiou A, Lebel T, Parker DJ, Polcher J. 2006. African Monsoon Multidisciplinary Analysis:

Copyright © 2009 Royal Meteorological Society

An international research project and field campaign. *Bull. Am. Meteorol. Soc.* **87**: 1739–1746.
Schumacher C, Houze RA Jr. 2003. Stratiform rain in the tropics as seen by the TRMM precipitation radar. *J. Climate* **16**: 1739–1756.
Schumacher C, Houze RA Jr. 2006. Stratiform precipitation production over sub-Saharan Africa and the tropical East Atlantic as observed by TRMM. *Q. J. R. Meteorol. Soc.* **132**: 2235–2255.
Schumacher C, Houze RA Jr, Kraucunas I. 2004. The tropical dynamical response to latent heating estimates derived from the TRMM Precipitation Radar. *J. Atmos. Sci.* **61**: 1341–1358.
Stephens GL, Wood NB. 2007. Properties of tropical convection observed by millimeter-wave radar systems. *Mon. Weather Rev.* **135**: 821–842.
Stephens GL, Vane DG, Boain RJ, Mace GG, Sassen K, Wang Z, Illingworth AJ, O'Connor EJ, Rossow WB, Durden SL, Miller SD, Austin RT, Benedetti A, Mitrescu C. 2002. The CloudSat mission and the A-TRAIN: A new dimension to space-based observations of clouds and precipitation. *Bull. Am. Meteorol. Soc.* **83**: 1771–1790.
Thorncroft C, Hodges K. 2001. African easterly wave variability and its relationship to Atlantic tropical cyclone activity. *J. Climate* **14**: 1166–1179.
Wang B, LinHo. 2002. Rainy season of the Asian–Pacific summer monsoon. *J. Climate* **15**: 386–398.
Webster PJ, Houze RA Jr. 1991. The Equatorial Mesoscale Experiment (EMEX): An overview. *Bull. Am. Meteorol. Soc.* **72**: 1481–1505.
Webster PJ, Stephens GL. 1980. Tropical upper-tropospheric extended clouds: Inferences from Winter MONEX. *J. Atmos. Sci.* **37**: 1521–1541.
Webster PJ, Bradley EF, Fairall CW, Godfrey JS, Hacker P, Houze RA Jr, Lukas R, Serra Y, Hummon JM, Lawrence TDM, Russell CA, Ryan MN, Sahami K, Zuidema P. 2002. The JASMINE pilot study. *Bull. Am. Meteorol. Soc.* **83**: 1603–1630.
Yuter SE, Houze RA Jr. 1995. Three-dimensional kinematic and microphysical evolution of Florida cumulonimbus. Part II: Frequency distribution of vertical velocity, reflectivity, and differential reflectivity. *Mon. Weather Rev.* **123**: 1941–1963.
Yuter SE, Houze RA Jr. 1998. The natural variability of precipitating clouds over the western Pacific warm pool. *Q. J. R. Meteorol. Soc.* **124**: 53–99.
Zuidema P. 2003. Convective clouds over the Bay of Bengal. *Mon. Weather Rev.* **131**: 780–798.

Copyright © 2009 Royal Meteorological Society

DOI: 10.1002/qj